中国光学（中英文） Chinese Optics 核心期刊

半导体白激光作为水下成像系统光源与单色激光、LED白光的对比成像实验

江子琦 刘晓梅 蔡夫鸿 张典 蔡惟玓 柳华

Imaging comparison experiment of an underwater imaging system with a semiconductor white laser, a monochromatic laser and an LED white light as the light source

JIANG Zi-qi, LIU Xiao-mei, CAI Fu-hong, ZHANG Dian, CAI Wei-yu, LIU Hua

引用本文:
江子琦, 刘晓梅, 蔡夫鸿, 张典, 蔡惟玓, 柳华. 半导体白激光作为水下成像系统光源与单色激光、LED白光的对比成像实验[J]. 中国光学, 2023, 16(2): 466−478. doi: 10.37188/CO.EN.2022−0012
JIANG Zi-qi, LIU Xiao-mei, CAI Fu-hong, ZHANG Dian, CAI Wei-yu, LIU Hua. Imaging comparison experiment of an underwater imaging system with a semiconductor white laser, a monochromatic laser and an LED white light as the light source[J]. *Chinese Optics*, 2023, 16(2): 466-478. doi: 10.37188/CO.EN.2022-0012

在线阅读 View online: https://doi.org/10.37188/CO.EN.2022−0012

文章编号 2097-1842(2023)02-0466-13

Imaging comparison experiment of an underwater imaging system with a semiconductor white laser, a monochromatic laser and an LED white light as the light source

JIANG Zi-qi[2], LIU Xiao-mei[1 *], CAI Fu-hong[1], ZHANG Dian[1], CAI Wei-yu[1], LIU Hua[1]

(1. *College of Mechanical and Electrical Engineering*, *Hainan University*, *Haikou* 570228, *China*;
2. *Fuzhou Vocational Technical College*, *Fuzhou* 344000, *China*)

* *Corresponding author*, *E-mail*: *liuxm@hainanu.edu.cn*

Abstract: To solve the problems of short illumination distance and narrow spectral range in the current underwater detection technology, an underwater semiconductor white laser imaging system was established. The quality of the images captured by the system under different light sources and different conditions was studied. A white laser with a power of 220 mW and a color temperature of 6 469 K synthesized by an RGB semiconductor laser is used as the underwater lighting source, which is respectively compared with three RGB monochromatic lasers and an LED white light source under different conditions. For these images, different algorithms are used to process, analyze and evaluate their quality. The results indicate that when the white laser is used as the underwater light source, the collected image is not only better than that with the LED white light source with respect to information detail and structural integrity, but also better than the monochrome laser in color reproduction of the target and the integrity of the edge feature information. The semiconductor white laser has the advantages of concentrated energy, strong color rendering, and high illuminance, and its light source performance can meet the requirements of underwater low-illumination imaging. With the same imaging system and imaging distance, images with stronger authenticity, better texture and more target feature information can be obtained.

Key words: laser display; semiconductor white laser; underwater laser imaging; underwater image processing

收稿日期:2022-07-22; **修订日期**:2022-08-03

基金项目:国家重点研发计划(No. 2018YFC1407503);国家自然科学基金地区科学基金项目(No. 61964006);海南大学科研启动基金项目(No. KYQD(ZR)1853)

Supported by National Key Research and Development Project (No. 2018YFC1407503); National Natural Science Foundation of China (No. 61964006); the Scientific Research Fund of Hainan University (No. KYQD(ZR)1853)

半导体白激光作为水下成像系统光源与单色激光、LED 白光的对比成像实验

江子琦[2], 刘晓梅[1*], 蔡夫鸿[1], 张　典[1], 蔡惟珏[1], 柳　华[1]
（1. 海南大学 机电工程学院，海南 海口 570228；
2. 抚州职业技术学院，江西 抚州 344000）

摘要: 为了解决现阶段开展水下探测工作时存在的照明距离短、光谱范围窄等问题, 建立了水下半导体白激光成像系统, 并对该系统在不同光源及不同条件下采集图像的质量进行分析。将基于红绿蓝(RGB)三基色半导体激光器合成的功率为 220 mW、色温为 6469 K 的白激光作为水下照明光源, 分别与红、绿、蓝三种单色激光及 LED 白光光源在不同条件下的水下成像效果进行对比。对于不同水下光源采集的图像, 使用不同算法对其进行处理、分析及质量评价。实验结果表明: 半导体白激光作为水下光源, 采集的图像不仅在细节信息及结构完整性上优于 LED 白光光源, 同时在目标物色彩还原度以及边缘特征信息完整度方面也优于单色激光。半导体白激光具有能量集中、显色性强、光照度高的优势, 其光源性能可满足水下低照度的成像要求, 在相同的成像系统及成像距离下可获得真实性更强、质感更好、目标物特征信息更多的图像。

关　键　词: 激光显示; 半导体白激光; 水下激光成像; 水下图像处理
中图分类号: O432.3　　**文献标志码:** A　　**doi:** 10.37188/CO.EN.2022-0012

1　Introduction

Since the advent of the semiconductor laser, the rapid development, many achievements, and wide applications make it almost occupy "half the sky" of the laser market. As an emerging laser light source, the white laser is an illumination light source technology that generates high-brightness white light through the laser[1-2]. The white laser has the advantages of wide frequency coverage, high brightness, high power peak value, strong directivity, a long working life, strong spatial and temporal coherence, etc. Therefore, it has played a practical role in scientific research and national defense, lighting display, communication information, medical testing, industrial production, and other fields[3-4].

With the increasing demand to detect and understand the ocean, the development of underwater laser imaging, underwater spectral analysis, underwater lighting, and other fields has grown rapidly[5-7]. At present, the light sources commonly used underwater imaging include LEDs, tungsten halogen lamps, and lasers. LED white light sources are widely used in underwater imaging and underwater target recognition due to their advantages of low cost, high luminous efficiency and long service life, but their energy is more divergent than laser light sources and their underwater transmission distance is shorter, so they are not suitable for underwater long-distance imaging and target recognition. Since seawater has much less blue-green light attenuation with wavelengths in the 470−580 nm band than other light bands, many countries have invested a lot of manpower and material resources in the application of blue-green lasers for underwater communication, detection, sensing, and other fields. Although blue-green lasers play an important role in applications such as underwater communication and detection, due to the limited spectral range of monochromatic lasers, blue-green lasers cannot be well used in underwater target recognition and spectral analysis[8-9]. The emergence of the semiconductor white laser provides a new development direction for the research of underwater light sources. Semiconductor

white lasers can not only cover the visible light spectrum, but also have relatively concentrated energy. Therefore, the application of a white laser in underwater imaging can not only overcome the narrow spectral range of monochromatic lasers, but also overcome the LED white light source energy divergence and short transmission distance. This is of great significance to the development of deep-sea detection technology and underwater laser imaging, and can better meet the application requirements of target imaging and identification for deep-sea detection instruments.

At present, due to limitations to the development of semiconductor lasers and the lack of in-depth research on synthetic white lasers, researches about white laser light sources used for underwater detection has not been carried out.

At the same time, due to the complexity of the water environment and the scattering and absorption of light in water, the underwater imaging quality is poor, which seriously limits the further development of underwater detection technology[10]. Underwater image processing technology can help improve image quality and effectively extract target information, which not only provides technical support for improving the performance of underwater target detection systems, but also provides reference directions for the image analysis of underwater white laser imaging.

In this paper, an underwater laser imaging system is built with a white laser used as the underwater lighting source with a power of 220 mW and a color temperature of 6469 K based on the red, green, and blue (RGB) three-primary laser synthesis, then a series of experiments are carried out. The purpose of the experiment is to explore whether the white laser can meet the working requirements of underwater laser imaging. Then, the underwater imaging effects of the white laser, the red, green, and blue monochromatic lasers, and the LED white light sources were compared under different underwater environments, different underwater imaging distances, and different targets. On this basis, we discuss whether three traditional image processing methods, namely median filtering, histogram equalization, and piecewise linear grayscale transformation, are suitable for underwater white laser imaging. At the same time, through the image processing and quality evaluation of underwater LED white light sources and white laser imaging, the superiority of underwater white laser imaging is verified.

2 Underwater imaging experiment system

2.1 Experimental principle

The experimental principle of using a camera to shoot underwater objects under a specific light source is shown in Figure 1. The underwater light source is fixed at the upper left corner of the water tank to ensure that all the light of the light source can be injected into the water, and the target is placed in the center of the water tank's bottom so that it can move in vertically. A ruler is used to measure the distance of the target from the water surface. The camera is positioned on the water and directly above the object to capture the image.

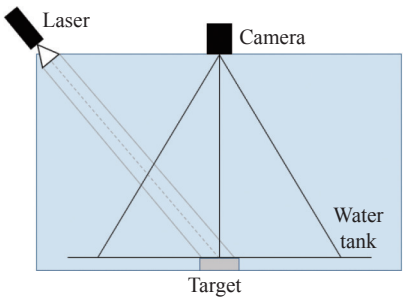

Fig. 1 Schematic diagram of the underwater laser imaging experiment

2.2 Experiment apparatus

The experimental instrument used in this paper is the LWRGB-F-FTP laser (LaserWave, China). It has the advantages of stable power, high beam quality, and convenient operation. It composed of power supply, laser head, optical fiber and lens barrel. The

white laser set up synthesized by an RGB semiconductor is shown in Figure 2.

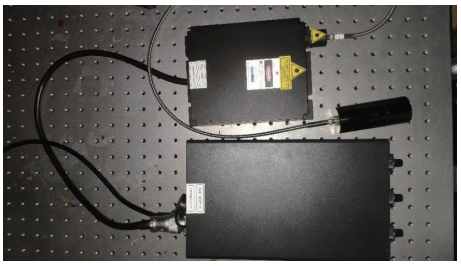

Fig. 2　Experimental setup for red, green and blue lasers

In this experiment, a 638-nm semiconductor red laser, 520-nm semiconductor green laser, and 445-nm semiconductor blue laser are used. After fiber coupling and output, the fiber core diameter is 400 μm. After the fiber is subjected to flat-top homogenization, a flat-top spot is obtained. The uniformity is larger than 70% and the angle is 29°. The lens barrel is connected to the optical fiber light outlet, and the light is finally emitted through the lens barrel. The optical parameters of the output white laser are tested by a spectral illuminometer (OHSP-350, Hopoocolor, China), and an optical power meter (LI-P50W, LaserWave, China) is used to measure the laser output power.

2.2.1　White laser

The white laser used in this paper is synthesized by three primary color lasers. The color temperature of the white laser is 6469 K, the color coordinates are (0.3199, 0.2805), and the power is 220 mW. The output spectrum of the white laser is shown in Figure 3 (color online).

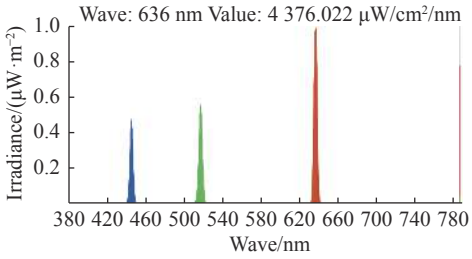

Fig. 3　Output spectrum of semiconductor white laser

2.2.2　Monochromatic lasers

The monochromatic lasers used in this paper includes red, green and blue primary color lasers. The color coordinates of the red laser are (0.7165, 0.2835) and the power is 260 mW; the color coordinates of the green laser are (0.0554, 0.8247) and the power is 120 mW; the coordinates of the blue laser are (0.1598, 0.0149) and the power is 330 mW. The output spectrum of the three primary color lasers are shown in Figures 4, 5 and 6.

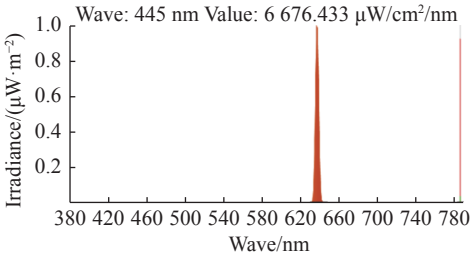

Fig. 4　Output spectrum of the semiconductor red laser

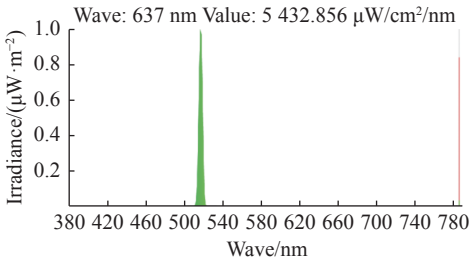

Fig. 5　Output spectrum of the semiconductor green laser

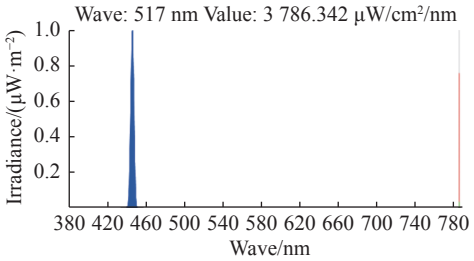

Fig. 6　Output spectrum of the semiconductor blue laser

The peak wavelengths corresponding to the three primary color lasers are 637.4 nm for the red light, 517.4 nm for the green light, and 446.6 nm for the blue light, respectively. Their spectral half-widths are 4.2, 4.5, and 4.0 nm, and the corresponding irradiances are 23.34, 17.45, 29.03 mW/cm^2.

2.2.3　LED white light source

The relevant optical parameters of the LED white light source used in this paper are shown in Table 1.

Tab. 1 Relevant optical parameters of the LED white light source

	LED1	LED2
Color temperature/K	7261	5846
Dominant wavelength/nm	477.9	518.9
Color rendering index/Ra	63	64.9
R proportion/(%)	11.7	11.8
G proportion/(%)	86.4	86.2
B proportion/(%)	1.8	2

2.2.4 Camera parameters

The shooting device used in this paper is a Huawei Honor P30 mobile phone, and the rear camera is used to shoot. The rear camera consists of three lenses: a 40-megapixel photosensitive lens, a 16-megapixel wide-angle lens, and an 8-megapixel telephoto lens.

2.3 Underwater image processing algorithm and image quality evaluation index

2.3.1 Underwater image processing algorithms

This paper mainly discusses the median filter method, histogram equalization, piecewise linear grayscale transformation, the MSRCR enhancement algorithm, and the Laplacian pyramid fusion method.

2.3.1.1 Median filter

This method can effectively reduce noise and eliminate abnormalities, especially for removing impulse noise interference. The principle is to establish a window, and the odd-numbered pixel values in the window are arranged in order of size, such as 3×3, 5×5, etc., and the median value of the window is taken to replace the gray value of the center point. In this paper, we will use 3×3, 5×5, 7×7, and 9×9 templates to perform median filtering on the collected images respectively.

2.3.1.2 Histogram equalization algorithm

The principle is to select the grayscale histogram of the original image and convert the more concentrated grayscale interval into a uniform distribution of all the grayscale intervals of the histogram. After the histogram is equalized, the grayscale range of the image is expanded, so the contrast is enhanced.

2.3.1.3 Piecewise linear grayscale transformation algorithm

The piecewise linear grayscale transformation algorithm maps the original image grayscale range 0~P to the transformed image grayscale range 0~Q through the transformation function and sets the original image function as $f(x, y)$, and the transformed image function as $g(x, y)$. If a given gray level range of the original image is $[a_0, b_0]$, and the given gray level range of the transformed image is $[a_1, b_1]$, then the transformation function is:

$$g(x,y)=\begin{cases}(a_1/a_0)f(x,y), 0\leqslant f(x,y)<a_0\\ [(b_1-a_1)/(b_0-a_0)][f(x,y)-a_0]+a_1,\\ a_0\leqslant f(x,y)\leqslant b_0\\ [(Q-b_1)/(P-b_0)][f(x,y)-b_0]+b_1,\\ b_0<f(x,y)\leqslant P\end{cases}. \tag{1}$$

When the values of a_0, b_0, a_1, b_1 change, the corresponding image processing results are also different. That is, when $a_0>a_1$, $b_0<b_1$, the original image gray level is expanded in the range of $[a_0, b_0]$, and $[0, a_0]$ and $[b_0, P]$ is compressed; when $a_0<a_1$, $b_0>b_1$, the gray level of the original image is expanded in the range of $[0, a_0]$ and $[b_0, P]$, and $[a_0, b_0]$ range is compressed. The image contrast can be increased through the above algorithm.

2.3.1.4 Image processing algorithms

The algorithm formula is as follow:

$$r(x,y)=\log R(x,y)=\log\frac{S(x,y)}{L(x,y)}, \tag{2}$$

where $R(x, y)$ represents the reflection property, $L(x, y)$ and $S(x, y)$ represent the incident light and the original image.

The application formula is expressed as follow:

$$r(x,y)=\log S(x,y)-\log[F(x,y)\oplus S(x,y)]. \tag{3}$$

Among them, $r(x, y)$ is the output image, $\oplus$ represents the convolution operation, and $F(x, y)$ is the center wrapping function.

$$F(x,y)=\lambda\cdot \mathrm{e}^{-\frac{x^2+y^2}{c^2}}, \tag{4}$$

where c is the Gaussian surround scale and λ is a constant.

The output images are weighted and averaged:

$$r(x,y)=\sum_{k}^{K}w_k\log S(x,y)-\log[F(x,y)\cdot S(x,y)] \quad . \tag{5}$$

Among them, K is the number of Gaussian centers, and multiple w_k are evenly distributed.

The output image is added with a color recovery factor $C(x, y)$:

$$C(x,y)=f[I_i'(x,y)]=\beta\log[\alpha I_i'(x,y)] \quad , \tag{6}$$

where $f(\cdot)$ is the mapping function, and α and β represent gain constants and nonlinear strengths.

2.3.1.5　Laplace pyramid fusion

The high-frequency and low-frequency signals are obtained by decomposing the image, and inversely transformation of the two signals are carried out to reconstruct the image, and finally, the image is obtained by fusion. The fusion formula is as follow:

$$R^l(x,y)=\sum_{k=1}^{K}G^l\{W^k(x,y)\}L^l\{I^k(x,y)\} \quad , \tag{7}$$

among them, l is the pyramid level, $L\{I\}$ is the Laplace transform of the input image I, and $G\{W\}$ is the normalized weight of the Gaussian distribution.

2.3.2　Image quality evaluation

The quality evaluation indicators used in this paper are Peak Signal-to-Noise Ratio (PSNR) and image structural integrity.

2.3.2.1　Peak signal to noise ratio

PSNR reflects the completeness of image detail information. The larger the value, the more complete the image information. The formula is as follow:

$$PSNR=20\cdot\lg\left(\frac{MAX_I}{\sqrt{MSE}}\right) \quad , \tag{8}$$

where MSE is the mean square error between the original image and the processed image, and MAX is generally 255.

2.3.2.2　Image structural integrity

Structural Similarity Image Integerity (SSIM) for short, the larger the value, the better the structural integrity of the image. The formula is as follow:

$$SSIM(x,y)=\frac{(2u_xu_y+C_1)(2v_xv_y+C_2)}{(u_x^2+u_y^2+C_1)(v_x^2+v_y^2+C_2)} \quad , \tag{9}$$

where u_x and u_y are the image's mean values, v_x and v_y are the image's standard deviations, and C_1 and C_2 are constants.

3　Underwater imaging experiments and results

The experiment was carried out in a dark field environment, and the ambient light intensity was less than 1lx. The experimental conditions are as follows: (1) underwater light sources are white laser; red laser; green laser; blue laser. (2) water quality: seawater, clear water; (3) underwater imaging distance: 5 cm, 19 cm; (4) underwater targets: oranges, safflowers, green leaves; (5) sink: 42 cm × 23 cm × 26 cm transparent glass sink.

The laser is fixed to the upper left corner of the water tank through the bracket, and the target is placed in the water tank, and it is in the center of the camera's field of view. Under varying conditions of seawater, clear water, and no water and the distance between the target and the water surface, a white laser and three monochromatic red, green, and blue lasers are used for contrast illumination respectively. The camera are adjusted to shoot objects at 5 cm and 19 cm underwater, and compare the lighting effects of the four light sources. The experimental process is shown in Figure 7 (color online).

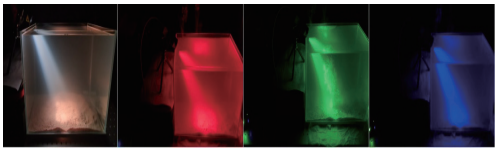

Fig. 7　Underwater lighting test with different light sources

When the water tank contains clear water, the images of different objects under different light sources and different imaging distances are collected, as shown in Figures 8–9 (color online).

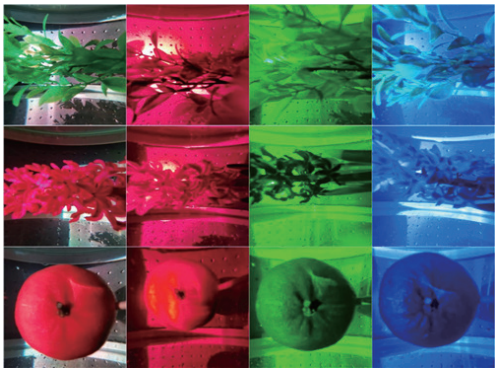

Fig. 8 The lighting effect of different light sources illuminating green leaves, safflower and oranges in clear water at a distance of 5 cm from the water surface

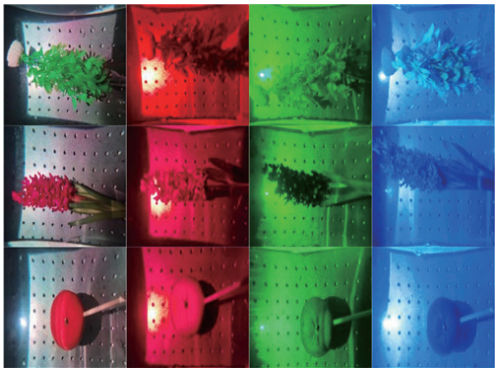

Fig. 9 The lighting effect of different light sources illuminating green leaves, safflower and orange targets in clear water at a distance of 19 cm from the water surface

When the water tank contains seawater, the images of different objects under different light sources and different imaging distances are collected, as shown in Figures 10−11 (color online).

Fig. 10 The lighting effects of different light sources illuminating green leaves, safflower, and oranges in seawater at a distance of 5 cm from the water surface

An image of the safflower at a distance of 19 cm from the sea water surface illuminated by the white laser in the above experiments was processed, and the applicability of the image smoothing processing based on median filtering and image enhancement using histogram equalization and piecewise linear grayscale transformation were discussed. The processing results are shown in Figures 12−14 (color online).

Based on the analysis of the images of differ-

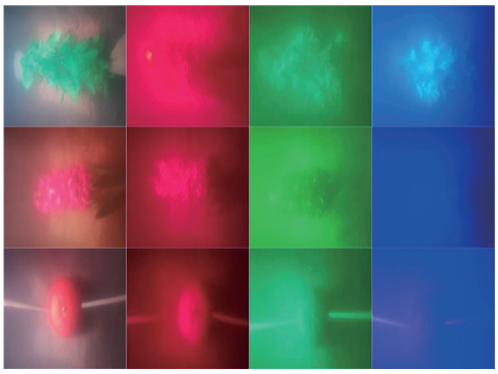

Fig. 11 The lighting effects of different light sources illuminating green leaves, safflower, and oranges in seawater at a distance of 19 cm from the water surface

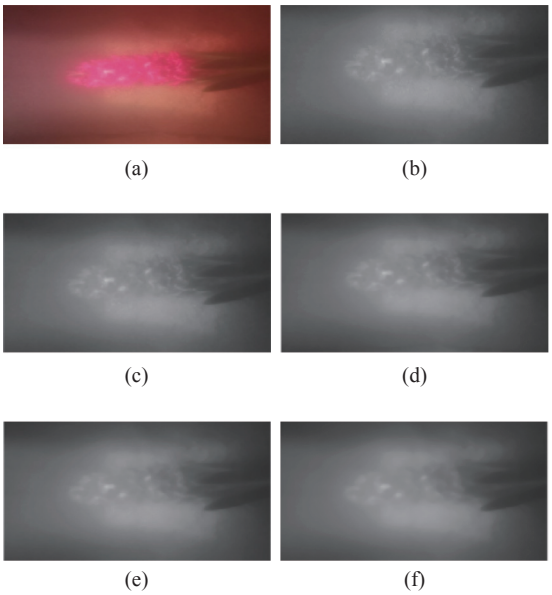

Fig. 12 Images of different size templates with the underwater imaging distance of 19 cm processed by median filter method. (a) Original image; (b) gray image; template processing results with (c) 3×3 window size; (d) 5×5 window size; (e) 7×7 window size; (f) 9×9 window size

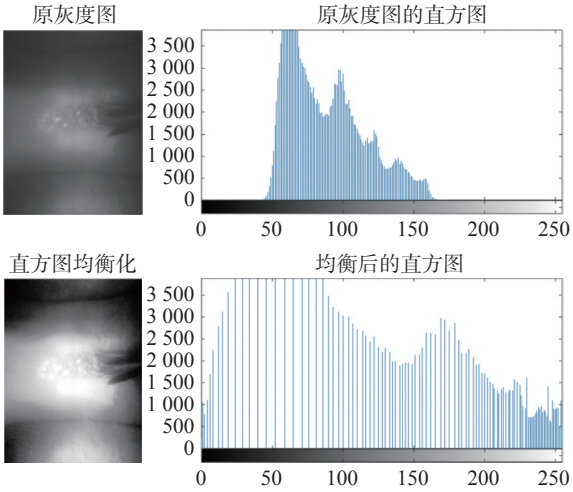

Fig. 13　Image processing results of the histogram equalization algorithm with an underwater imaging distance of 19 cm

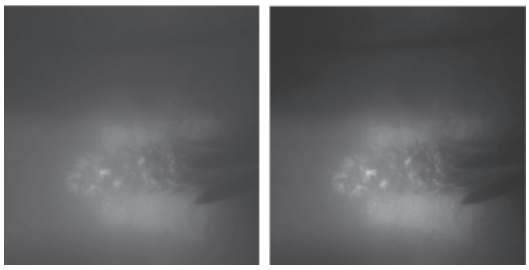

Fig. 14　Original image (left) and processing results (right) of piecewise linear grayscale transformation of underwater imaging at a distance of 19 cm

ent objects illuminated by different light sources at different underwater imaging distances in clear water and seawater, we can derive the following conclusions:

(1) Under the same underwater imaging distance and camera parameters, the color reproduction of the images illuminated by the white laser light source is higher than that of the images illuminated by the red, green, and blue lasers.

(2) When the imaging distance is long, the color of the object illuminated by the white laser is still clearly visible, while the color and edge information of the object under other light sources are difficult to identify.

(3) Due to a large number of particles and impurities in seawater and the complex water environment, the quality of the images obtained in seawater is not as good as the images in clear water.

(4) These three kinds of image processing methods can improve the image contrast to a certain extent, but as the underwater imaging distance increases, the image edge information will also be blurred.

The experimental results show that the illumination effect of the white laser for underwater laser imaging is better than that of the red, green, and blue monochromatic lasers.

4　Contrast experiment of underwater imaging

In the underwater laser imaging system built in Section 3, image acquisition is performed after changing certain experimental conditions. The transformed experimental conditions are as follows:

(1) Underwater light source: white laser with an output power of 220 mW and color temperature of 6 469 K; LED1 with an output power of 234 mW and color temperature of 7 261 K; LED2 with an output power of 242 mW and color temperature of 5 846 K;

(2) Water quality: seawater, clear water;

(3) Underwater imaging distance: 15 cm, near the water surface;

(4) Underwater target: target A- small wheel, target B- breakfast milk;

(5) Sink: 42 cm × 23 cm × 26 cm transparent glass sink.

The laser is fixed to the upper left corner of the water tank through the bracket, and the target is placed in the water tank and is in the center of the camera's field of view. The distance between the target and the water surface are changed with a white laser and two LED white light sources for contrast illumination. Adjust the parameters of the camera to be consistent, shoot underwater objects at 15 cm and near the water surface, and compare the lighting effects of the light source. The experimental process is shown in Figures 15 and 16 (color online).

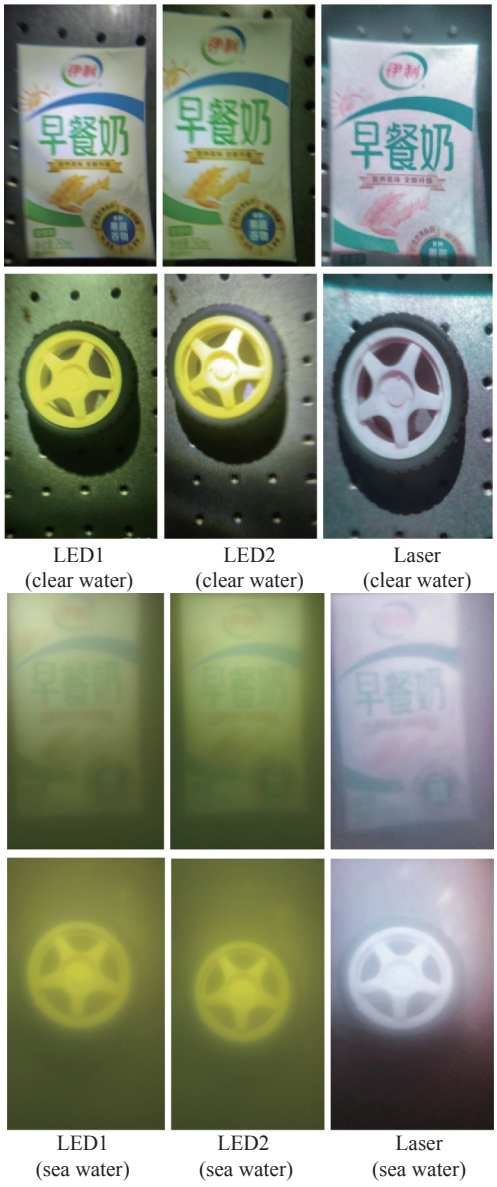

Fig. 15 Imaging results with different light sources when the underwater imaging distance is 15 cm in clear water and seawater

In Figures 15−16, the images obtained with different light sources LED1, LED2, and white laser in seawater are processed through histogram equalization enhancement AHE, Laplace pyramid fusion, and the MSRCR color restoration algorithm. The processing results are shown in Figures 17−19 (color online).

After analyzing the above processing results, it is subjectively believed that in terms of processing effect, Laplacian Pyramid Fusion is better than Histogram Equalization AHE and Histogram Equalization AHE is better than MSRCR Color Restoration Algorithm.

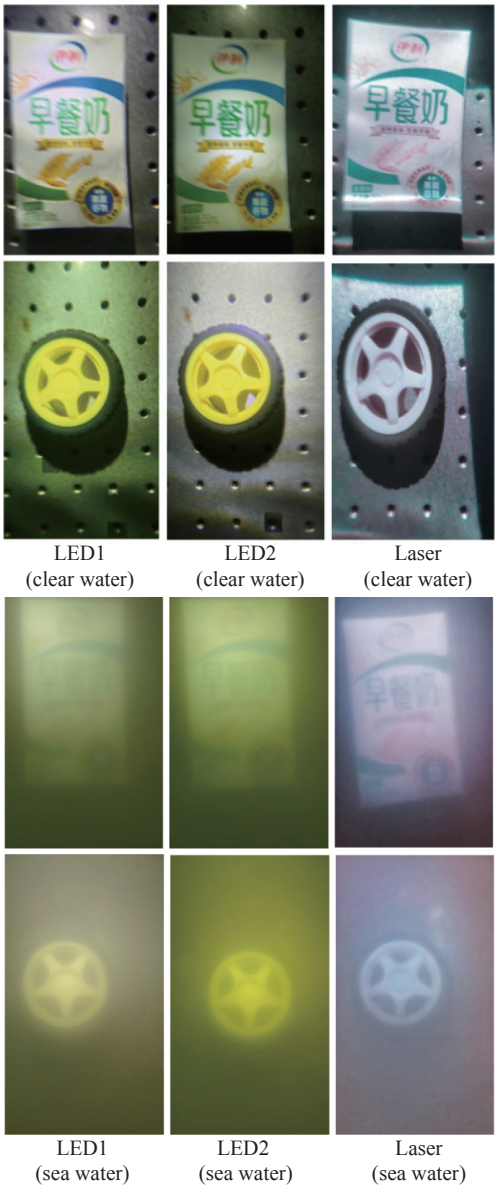

Fig. 16 Imaging with different light sources near the water surface in clear water and seawater

We recorded the image quality parameters after the Laplacian pyramid processing at this time, and on this basis, for the image processed by the Laplacian pyramid, image enhancement is performed by the contrast limited adaptive histogram equalization method (“CLAHE” for short). The image quality evaluation was implemented for the processing results of each step, and the underwater imaging performance of the white laser and the LED white light source was compared and analyzed. The flowchart of the image processing and evaluation method is

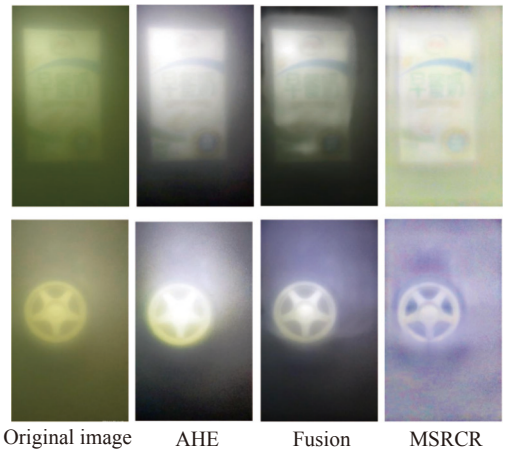

Fig. 17　Image processing results obtained with the light source LED1 in seawater imaging on the water surface

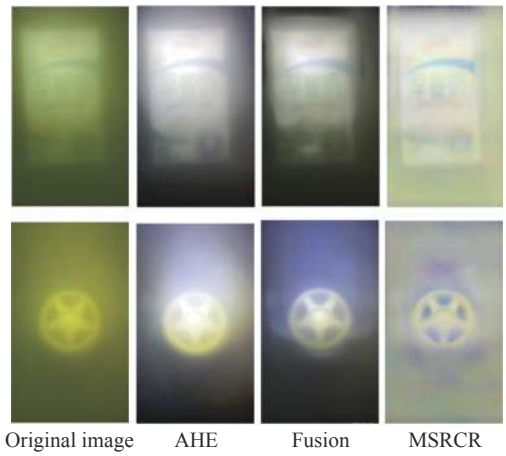

Fig. 18　Image processing results obtained with the light source LED2 in seawater imaging on the water surface

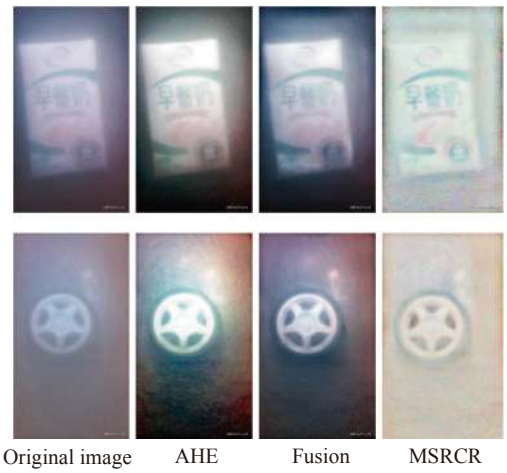

Fig. 19　Image processing results obtained with the light source white laser in seawater imaging on the water surface

shown in Figure 20.

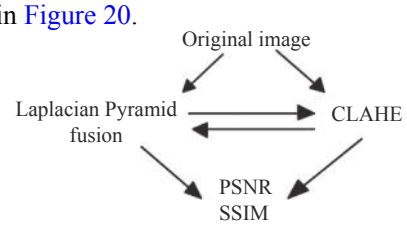

Fig. 20　Image processing and evaluation method

The processed results are shown in Figures 21 and 22 (color online).

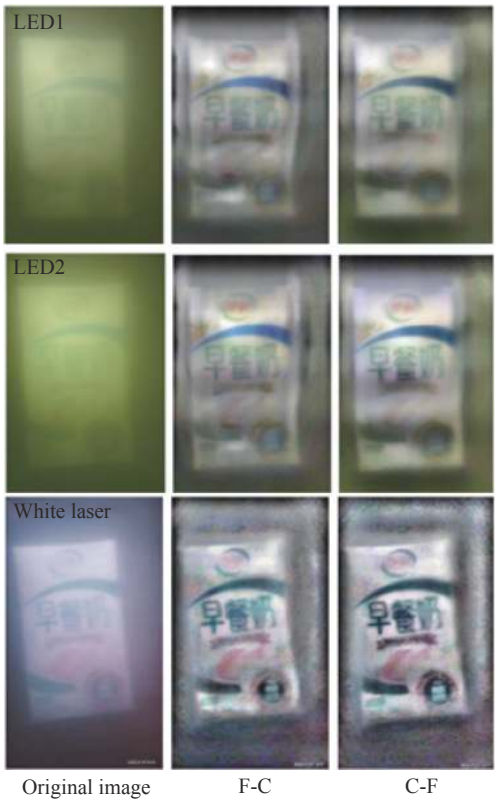

Fig. 21　Image processing results of object A taken near the water surface under different white light sources in seawater

The quality of above processed images are evaluated, and the quality evaluation indicators are PSNR and SSIM. The results are shown in Tables 2 and 3.

By analyzing the images, we can conclude:

(1) Comparing the images under different light sources and different water qualities, it can be found that the seawater has more particles and impurities and the water environment is more complex, resulting in the quality of the taken images is not good as the images in the clean water environment. When

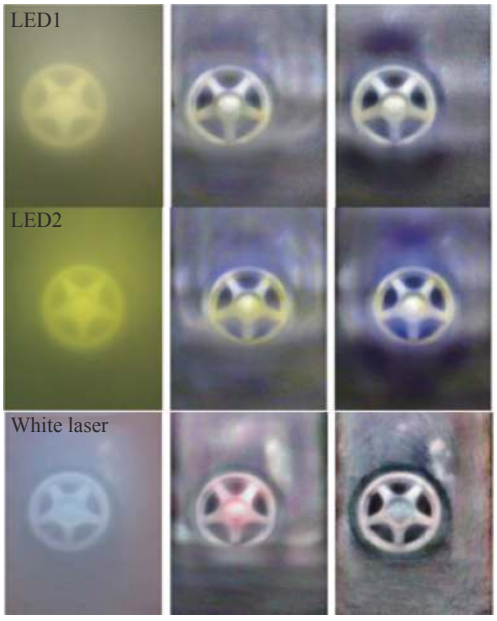

Fig. 22 Image processing results of object B taken near the water surface under different white light sources in seawater

Tab. 2 Results of Peak Signal to Noise Ratio (PSNR)

	LED1 object A/B	LED2 object A/B	white laser object A/B
CLAHE	12.8346/14.5588	13.1192/16.5358	20.1845/20.4774
Laplacian Pyramid Fusion	18.9785/17.0071	17.8455/13.0359	19.0232/18.9562
F-C	12.2237/12.9728	12.3596/11.9641	17.0214/17.6895
C-F	12.0095/11.7048	11.5700/10.8762	17.1908/16.0493

Tab. 3 Results of Structural Similarity Image Integnity（SSIM）

	LED1 object A/B	LED2 object A/B	white laser object A/B
CLAHE	0.8416/0.7122	0.7904/0.8709	0.8230/0.9070
Laplacian Pyramid Fusion	0.9279/0.9251	0.9249/0.9291	0.9465/0.9398
F-C	0.8088/0.6590	0.7510/0.8058	0.7550/0.8749
C-F	0.8271/0.5615	0.7610/0.7392	0.7687/0.8184

the LED white light is imaged in the underwater environment, there is a sudden drop in optical power. The propagation path of the LED white light is more divergent than that of the white laser, the attenuation effect of the water body is stronger, and the light scattering reaction is more serious. As a result, the image quality of white light in underwater environment becomes worse. The utilization efficiency is low, the image presented is relatively blurred and brightly exposed, and some of the characteristic information of the target is lost.

(2) By comparing image qualities under different light sources and different imaging distances, it can be found that when the imaging distance is long, the feature information of the target under white laser illumination is still clearly visible, while the color and edge information of the target under an LED white light source and other features have been difficult to identify.

To summarize, the illumination effect of a white laser light source for underwater laser imaging is better than that of an LED white light source.

By analyzing the PSNR and SSIM values in Table 2 and Table 3, we can conclude:

(1) By comparing the PSNR and SSIM values under the white laser and the white LED light source, it can be found that the value under the white laser is larger, indicating that the white laser is better than the LED white light in terms of retaining image details and image structure integrity;

(2) By comparing the values of objects A and B under the two light sources, it can be found that there are differences in the values, and the difference under the white laser light source is smaller than that under the LED white light source, indicating that the laser light source has a stronger ability to store target information and the imaging robustness under the laser light source is stronger;

(3) By comparing the performances of the four image processing methods for underwater images under white laser, it is found that the PSNR value of the image processed by CLAHE is the largest, indicating that this method maximizes the feature and detail information of the image to the maxmum extent. The SSIM value of the image processed by the Laplacian pyramid fusion method is the largest, indicating that this method is good at preserving image features and highlighting edge information.

From the above analysis results, it can be concluded that the white laser light source is more suitable for underwater imaging than the LED light

source.

5 Conclusion

According to the principle of underwater laser imaging, the white laser light source synthesized by red, green, and blue semiconductor lasers is used as an underwater light source to realize the image acquisition of underwater imaging, which provides a new direction for the research of underwater lighting sources. With red, green, and blue monochromatic lasers and LED white light sources as the contrast light source, the underwater lighting effect test experiment was carried out. The experimental results show that the white laser has high color reproduction, a long imaging distance, and richer target image information under underwater imaging condition. It proves the superiority of the white laser as an underwater illumination source. In addition, when the white laser beam combined with the semiconductor three-primary laser beams is used as the light source of the underwater detection system, it can not only be used as a white light source, but also can be easily realized by controlling the output of three single-color lasers and using only a single-color laser for illumination. The mutual switching between the color light source and the white light source is conducive to promoting the multi-functional compatibility and performance expansion of the underwater detection system, and is of great significance to the development of deep-sea detection technology. The combined semiconductor beam and white laser light source has both the advantages of monochromatic laser transmission distance and the spectral advantages of LED white light sources, and is a new research direction of underwater lighting.

References:

[1] YANG Y, ZHUANG S L, KAI B C. High brightness laser-driven white emitter for Etendue-limited applications[J]. *Applied Optics*, 2017, 56(30): 8321-8325.

[2] CANTORE M, PFAFF N, FARRELL R M, *et al*.. High luminous flux from single crystal phosphor-converted laser-based white lighting system[J]. *Optics Express*, 2016, 24(2): A215-A221.

[3] 田景玉. 高功率半导体激光器外腔合束技术及白激光研究[D]. 长春: 中国科学院大学(中国科学院长春光学精密机械与物理研究所), 2019.
TIAN J Y. Research on high power diode laser external cavity beam combination and white laser[D]. Changchun: Changchun Institute of Optics, Fine Mechanics and Physics, Chinese Academy of Sciences, 2019. (in Chinese)

[4] 吕伟振, 刘伟奇, 张大亮. 激光与LED混合投影光源色度学特性分析[J]. 液晶与显示, 2015, 30(2): 369-373.
LV W ZH, LIU W Q, ZHANG D L. Colorimetric analysis of laser and LED hybrid projection sources[J]. *Chinese Journal of Liquid Crystals and Displays*, 2015, 30(2): 369-373. (in Chinese)

[5] 何赛灵, 李硕, 陈祥, 等. 高光谱图谱仪与激光雷达及其在海洋生物检测方面的应用[J]. 红外与激光工程, 2021, 50(6): 20211033.
HE S L, LI SH, CHEN X, *et al*.. Application of hyperspectral imager and lidar in marine biological detection[J]. *Infrared and Laser Engineering*, 2021, 50(6): 20211033. (in Chinese)

[6] 唐耿彪, 张巍, 关夏威. 水下激光成像系统分辨率自动检测算法研究[J]. 舰船电子工程, 2021, 41(10): 170-173,183.
TANG G B, ZHANG W, GUAN X W. Research on resolution automatic detection algorithm of underwater laser imaging system[J]. *Ship Electronic Engineering*, 2021, 41(10): 170-173,183. (in Chinese)

[7] 孙鹏. 水下光学成像技术及应用[J]. 科学技术创新, 2021(16): 53-54.
SUN P. Underwater optical imaging technology and application[J]. *Scientific and Technological Innovation*, 2021(16): 53-54. (in Chinese)

[8] 叶庆, 范一松, 卞进田, 等. 适用于水下同步照明的灯泵浦绿光激光器研制[J]. 光子学报, 2018, 47(11): 1114004.
YE Q, FAN Y S, BIAN J T, *et al*.. Development of a green laser pumped by flash lamp applicable to underwater synchronous lightening[J]. *Acta Photonica Sinica*, 2018, 47(11): 1114004. (in Chinese)

[9] 梁赫西, 沈天浩, 王振亚, 等. 双光源水下无线光通信系统的研究与实现[J]. 红外与激光工程, 2021, 50(9): 20200445.

LIANG H X, SHEN T H, WANG ZH Y, *et al*.. Research and design of underwater wireless optical communication system with dual light sources[J]. *Infrared and Laser Engineering*, 2021, 50(9): 20200445.(in Chinese)

[10] 张卓, 张学武, 石孙凤, 等. 基于红蓝通道先验主动光源偏振水下图像复原算法[J]. 计算机测量与控制, 2022, 30(9).

ZHANG ZH, ZHANG X W, SHI S F, *et al*.. Underwater image restoration algorithm based on red and blue channel prior active light source polarization[J]. *Computer Measurement & Control*, 2022, 30(9).(in Chinese)

Author Biographics:

JIANG Zi-qi (1996—), female, born in Fuzhou, Jiangxi Proxince, obtained her master's degree from Hainan University in 2021, mainly engaged in the synthesis of semiconductor laser white light sources, underwater imaging, etc. E-mail: 474972775@qq.com

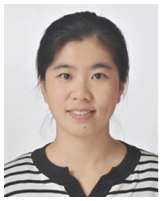

LIU Xiao-mei(1981—), Ph.D., female, born in Changchun, Jilin province, lecturer, received a bachelor degree from Changchun University of Science and Technology in 2004 and a doctorate degree from the University of Chinese Academy of Sciences in 2013. She is currently a teacher at the School of Mechanical and Electrical Engineering of Hainan University, mainly engaged in imaging spectroscopy, opto-mechanical integration. E-mail: liuxm@hainanu.edu.cn